The Effects of Violin Varnish on the Acoustic Properties of *Picea Engelmannii*

Mathias Hudoba de Badyn

Mentor: Professor Mark Van Raamsdonk

Science One 2010/11

The University of British Columbia

Vancouver, Canada

April 2011

Abstract:

Acoustic spectral analysis was performed on plates of *Picea Engelmannii* (Engelmann Spruce) before and after application of one of 3 types of varnish. The first overtone of each sample was driven through tapping by hand, and analyzed through a Fast Fourier Transform algorithm. The resulting acoustic spectrum was used to determine the frequency, quality factor Q, attenuation rate α and damping coefficient ζ changes as a result of the varnish application. A colophony-linseed oil and shellac-spirit varnish, and polyester lacquer were tested. A formula for predicting frequency shift based on mass and thickness of varnish added was determined, and varying trends of Q, α and ζ were reported. Wave propagation and the plate mechanics were analyzed.

1 Introduction

The violin is a musical instrument that is considered to have been perfected in part by the Italian violinmakers in the early 1700's. All methods of making violins today have not deviated from the design created by these makers. A significant mystique surrounds the idea of violin varnish, since none of the prominent makers such as Antonio Stradivari kept records of their varnish recipies. Some claim the effect of varnish on the violin to be the source of many positive acoustic properties. We present here a quantitative approach that determines the effect of three kinds of musical instrument finishes through measurements of the frequency spectrum, quality factor, decay rate and damping coefficients of plates of wood with and without varnish.

Violin varnish, and indeed any type of wood finish, consists of a solute dissolved in a solvent. When applied to the wood, the solvent is spontaneously removed either through oxidation, catalysis or vaporation, leaving behind the hard solute. The properties of the deposited solute are hypothesized to impart an effect on the acoustic properties.

Two types of varnish and one type of lacquer were tested. The first is a linseed oil-based varnish, which uses colophony as the solute, and boiled linseed oil as the solvent. Dessicated *Aloe vera* was added as a colourant. Colophony is the product of removing terpenes from raw pine resin, and consists of mostly abietic acid ($C_{20}H_{30}O_2$; see Fig. 1.1), with mixed proportions of other resin acids and impurities. Linseed oil is extracted from linseed, otherwise known as flaxseed. It consists mainly of linoleic acid ($C_{18}H_{32}O_2$; see Fig. 1.1), a relatively polar molecule which allows colophony to dissolve readily. This finish penetrates into the wood, and intercalates between cellulose strands. The surface of the varnish is very soft and malleable.

The second type of varnish tested was a shellac-spirit varnish. Shellac is the purified excrement of the lac beetle. It is a natural polymer, and thus has properties similar to hard plastics and is soluble in alcohol. A 75% isopropyl alcohol solution was used to dissolve the raw shellac, which comes in thin flakes on the order of 1 cm in diameter. Shellac-based finishes have very little wood penetration, and rest almost chiefly on the surface of the wood. They are of medium stiffness, however cure hard over long periods of time.

The final finish tested was a commercial polyester lacquer[1]. As a commercial product, its exact composition was unknown, however several properties apply to most polyester finishes. They are usually cured through catalysis with methyl ethyl ketone peroxide ($C_8H_{18}O_6$; see Fig 1.1), and are considered to be very stiff compared to most finishes, and also have very little wood penetration.

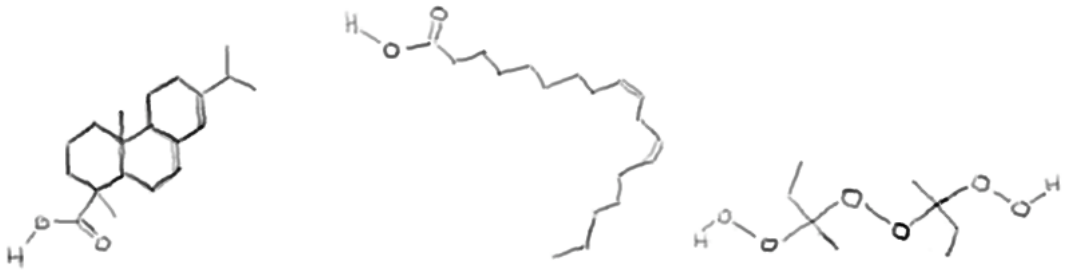

[1]This finish was kindly donated by David Webber of Webber Guitars. To protect his commercial interests, the exact brand name of the finish was excluded from this paper.

Figure 1.1: Structural diagrams of abietic acid, linoleic acid and methyl ethyl ketone peroxide, respectively. Redrawn from information accessed from www.wolframalpha.com in March 2011.

2 Methods

20 2-year old pieces of Engelmann Spruce from a single tree felled in Revelstoke, BC., were cut into 4.5" by 10.5" pieces with thickness ranging from 2mm to 3mm, with the grain running parallel to the long side. To measure the frequency spectrum, sound clips of the wood vibrating at a resonant frequency were recorded. The measured mode is shown in Fig. 2.1. Nodal lines are located approximately at one-quarter and three-quarters of the length.

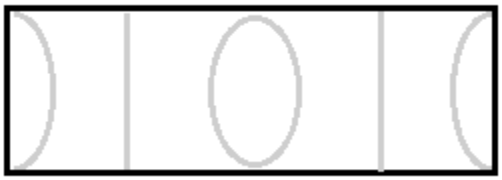

Figure 1.1: The nodes and antinodes of a rectangular plate at the measured mode. Lines represent nodes, ovals represent regions of high oscillations.

The sound clips were recorded using a studio-quality microphone through an Alesis i0-14 mixer system. The microphone was placed in a box lined with 3 inches of insulating foam glued with liquid foam, and was suspended using a bungee cord damper to prevent noise propagating through the ground. The box was covered in aluminum foil to prevent electrostatic interference. Holes were cut on either side of the box to faciliated holding the pieces of wood while recording. Samples of wood were held at a node and tapped in the central antinode to induce a resonance, which was recorded using Audacity at a sampling rate of 8000 Hz. Twenty taps were recorded for 30 pieces of wood. A Fast Fourier Transform algorithm was used to extract the frequency spectrum for each tap. The Nyquist frequency for this sampling rate is 4000 Hz, which is the highest frequency that can be resolved without aliasing. Only frequencies < 1000 Hz were analyzed. The masses and thicknesses of the wood were measured to calculate average sample densities.

Three treatments of colophony-linseed oil violin varnish were made by boiling 300 mL Western Family brand linseed oil and dissolving 100 g, 120 g and 150 g of colophony, and 75 g *Aloe vera* powder in each. The shellac-spirit varnish was made by dissolving 100 g, 125 g and 150 g of shellac in 500 ml 75% isopropyl alcohol, with mild heat applied through a hot water bath as necessary. These varnishes were applied to the wood in 2-3 coats, with five pieces assigned to each treatment. Masses were recorded to measure the amount of varnish added, and the frequency spectrum was recorded as described in the preceding paragraph. David Webber finished the pieces assigned to test the polyester guitar finish according to his own protocol.

The quality factor Q is defined to be $\frac{f_0}{\Delta f}$ where f_0 is the maximum value of the peak, and Δf is the width of the peak in the frequency spectrum at half the energy of the maximum of the peak. In terms of decibels, this corresponds to the width of the peak at 3.01 dB below the maximum. These values were determined by linear or polynomial extrapolation from the frequency spectrum.

The attenuation α of the oscillation is derived to be $\frac{\pi f_0}{Q}$, and is an inverse measure of how much input energy is outputted as sound energy. Finally, the damping coefficient ζ is $\frac{1}{2Q}$, which is used to model the plate vibration using a set of differential equations and is a measure of the damping of the plate oscillation.

3 Results - Colophony-Linseed Oil Varnish

The three treatments were not significantly different from one another, so they were modelled as one single treatment. Error was progagated through measurements using standard error propagation formulae (see Appendix).

Figure 3.1 shows that frequency shift is negatively correlated with the mass of varnish added to the wood. Similar effects are shown with the change in average sample density. This correlation is statistically significant, and was used to construct a model as shown later. The average frequency shift was -17.6767 Hz± 0.7004, where the uncertainty is the standard error (see Appendix).

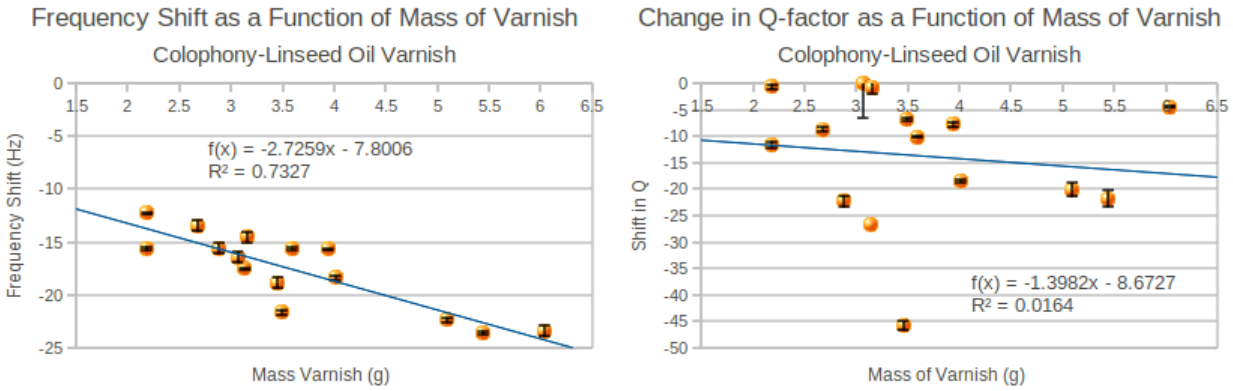

Figures 3.1 and 3.2: Δf and ΔQ as functions of mass of varnish. Error bars represent propagated uncertainty.

The change in Q (Fig. 3.2) from varnished samples to unvarnished samples was not correlated well, although in almost all cases a negative ΔQ was recorded. The shifts in α and ζ are calculated using Q, so they too are not correlated well. A positive shift in α was seen in most samples, however the shift was smaller as more varnish was added. Despite the lack of correlation, the results are statistically significant, as there are error bars that do not overlap. The shift in ζ is largely insignificant.

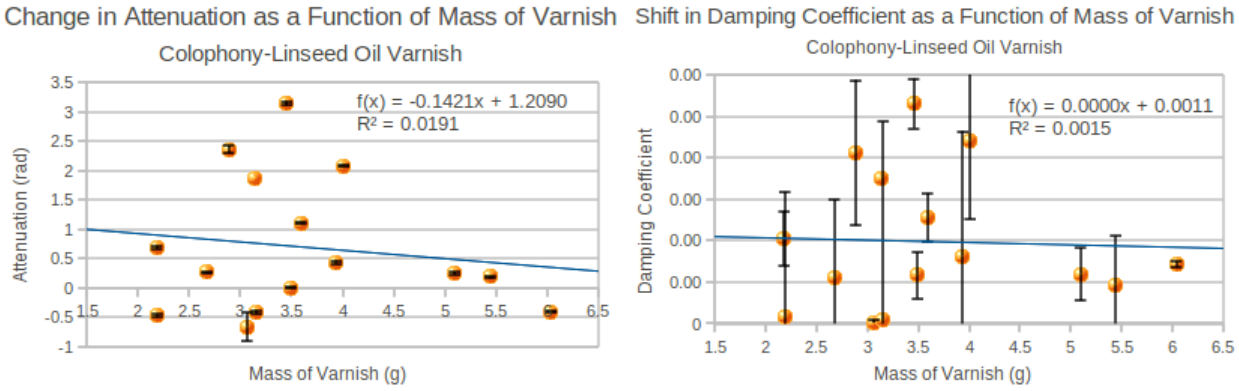

Figures 3.3 and 3.4: $\Delta\alpha$ and $\Delta\zeta$ as functions of the mass of varnish. Error bars represent propagated uncertainty.

In Fig. 3.5, the ratio of varnished to unvarnished sample frequencies $\frac{f}{f_0}$ was graphed as a function of varnished and unvarnished average sample densities $\frac{d}{d_0}$. A strong negative linear correlation, was shown. The following three formulae were empirically deduced by analyzing the data, and finding strong trends.

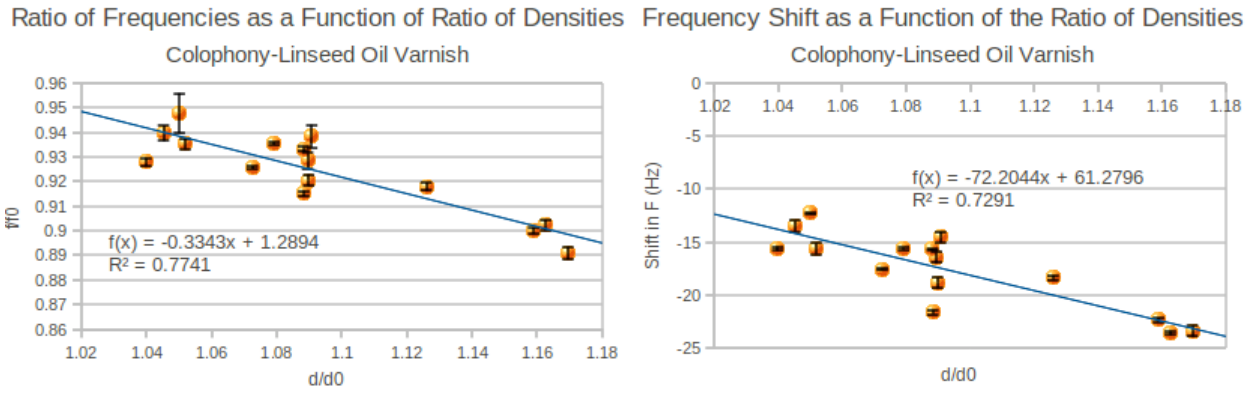

Figures 3.5 and 3.6: $\frac{f}{f_0}$ and Δf as functions of $\frac{d}{d_0}$. Error bars represent propagated uncertainties.

This implies that

$$f \propto \lambda_1 f_0 \frac{d}{d_0} \tag{1}$$

where $\lambda_1 = -0.3343$ is the proportionality constant.

In Fig. 3.6, the frequency shift $\Delta f = f - f_0$ was plotted against $\frac{d}{d_0}$ to produce yet another negative correlation, giving the proportionality

$$f \propto f + \lambda_2 \frac{d}{d_0} \tag{2}$$

with the constant $\lambda_2 = -72.2044\,\text{Hz}$.

Farag and Pan (1998) presented a mathematical model of predicting the fundamental frequencies of a rectangular plate of constrained edges and thickness h, which can be used to model, for example, a rectangular guitar soundboard glued to the sides:

$$f_0 = \frac{1}{2\pi}([(\frac{m\pi}{a^2}) + (\frac{n\pi}{b^2})] \times \sqrt{\frac{D}{d_0 h}}), \tag{3}$$

$$\omega_0 = [(\frac{m\pi}{a^2}) + (\frac{n\pi}{b^2})] \times \sqrt{\frac{D}{d_0 h}} \tag{4}$$

With some algebra, a formula for frequency shift can be derived:

$$\frac{\omega_2}{\omega_1} = \frac{\sqrt{\frac{D}{d_2 h_2}}}{\sqrt{\frac{D}{d_1 h_1}}} = \sqrt{\frac{d_1 h_1}{d_2 h_2}} \tag{5}$$

giving

$$f_2 = f_1 \sqrt{\frac{d_1 h_1}{d_2 h_2}} \tag{6}$$

where h_1 is the thickness of the plate before varnishing, h_2 is the thickness after varnishing, and d_1 and d_2 are the densities of the plate before and after varnishing.

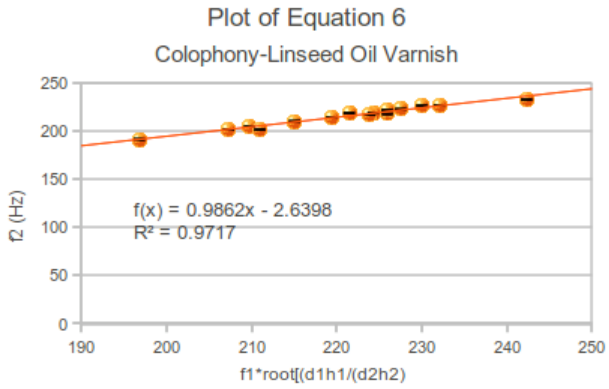

Figures 3.7: Equation 6: predicted frequency shifts plotted against measured frequencies. Error bars represent uncertainty in the measured frequency.

The linear regression results in a line extremely close to $y = x$, meaning that the equation derived gave predicted values almost identical to the values obtained experimentally.

4 Results - Shellac-Spirit Varnish

The results for the shellac-spirit varnish were similar to that of the colophony-linseed oil varnish, and again the three treatments did not deviate from each other significantly and were modeled as one treatment.

Fig. 4.1 shows the relationship between frequency shift and the mass of varnish added. The graph shows a statistically significant negative trend with an increased negative frequency shift as more varnish is added with low correlation. The average frequency shift was $-5.0134\,\text{Hz} \pm 0.2467$, where the uncertainty is the standard error (see Appendix). The plot of Q with mass of varnish added shows a significant negative trend, but little correlation.

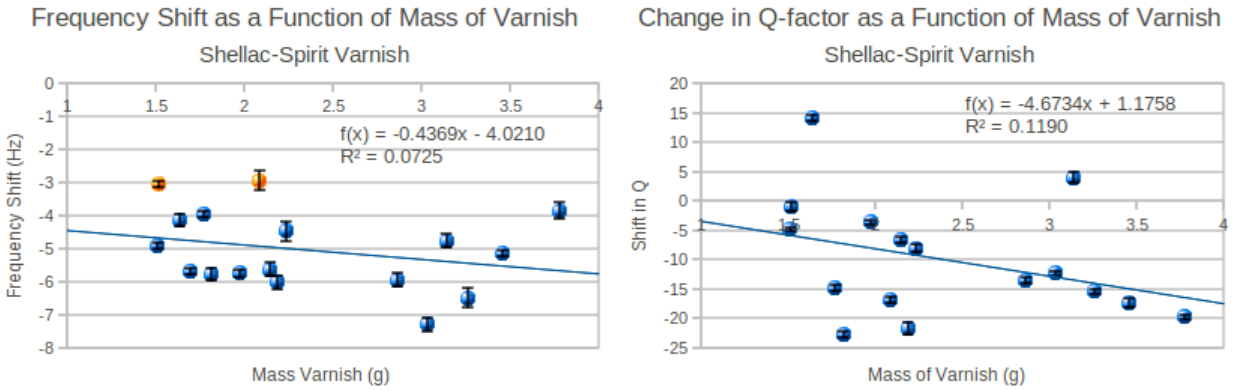

Figures 4.1 and 4.2: Δf and ΔQ as functions of mass of varnish. Error bars represent propagated uncertainty.

In Fig. 4.3 and 4.4, α and ζ are correlated with the mass of varnish added better than the colophony-linseed oil varnish, and show a significant positive trend.

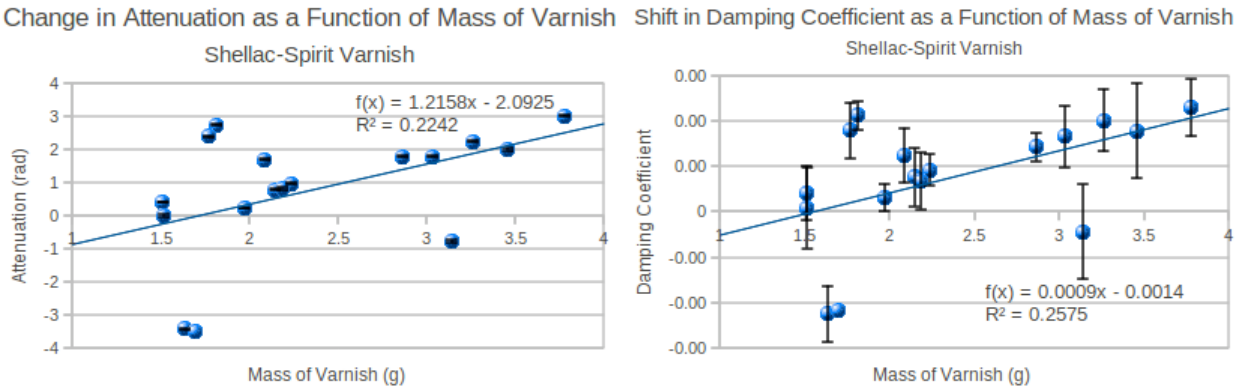

Figures 4.3 and 4.4: $\Delta\alpha$ and $\Delta\zeta$ as functions of the mass of varnish. Error bars represent propagated uncertainty.

The graph for the unvarnished to varnished frequencies $\frac{f}{f_0}$ as a function of the unvarnished to varnished densities $\frac{d}{d_0}$ shows a significant, positively correlated plot in contrast to that of the colophony-linseed oil varnish, as does the plot for $\Delta f = f - f_0$ as a function of $\frac{d}{d_0}$.

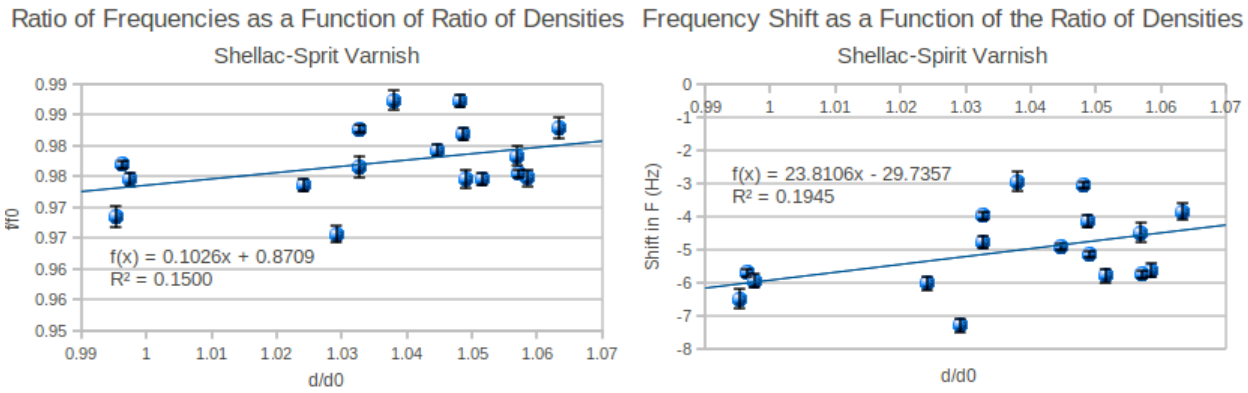

Figures 4.5 and 4.6: $\frac{f}{f_0}$ and Δf as functions of $\frac{d}{d_0}$. Error bars represent propagated uncertainties.

Both these graphs suggest the same proportionalities as the colophony-linseed oil varnish:

$$f \propto \lambda_3 f_0 \frac{d}{d_0}, \tag{7}$$

$$f \propto f + \frac{\lambda_4 d}{d_0}, \tag{8}$$

where λ_3 and λ_4 are proportionality constants. As for the colophony-linseed oil varnish, the derived equation 6 was plotted:

$$f_2 = f_1 \sqrt{\frac{d_1 h_1}{d_2 h_2}}. \tag{9}$$

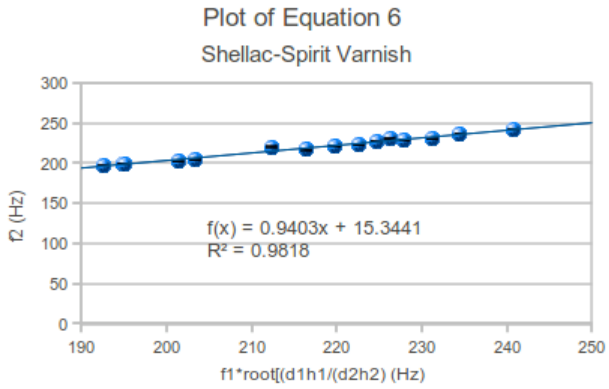

Figures 4.7: Equation 6: predicted frequency shifts plotted against measured frequencies. Error bars represent uncertainty in the measured frequency.

Again, the plot gives a linear regression close to $y = x$, although a larger intercept is seen with this stiffer varnish.

5 Results - Polyester Guitar Lacquer

In Fig 5.1, equation (6) was plotted using the data obtained from testing the polyester finish from Webber Guitars.

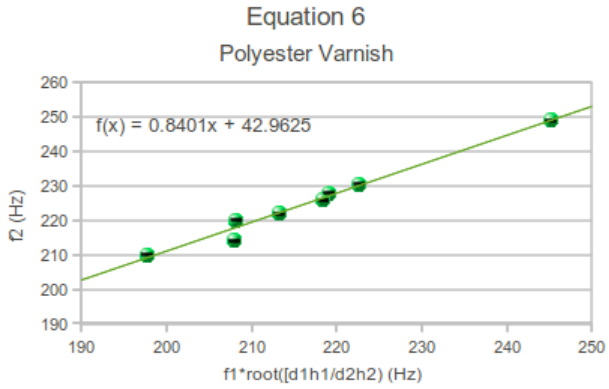

Figure 5.1: Equation 6: predicted frequency shifts plotted against measured frequencies. Error bars represent uncertainty in the measured frequency.

This plot does not show a line close to $y = x$. In the discussion, this is thought to be caused by the stiff varnish acting as a separate joined plate.

6 Discussion

The results from both the shellac-spirit varnish and the colophony-linseed oil varnish experiment provide several conclusive results. Both varnishes showed a negatively correlated trend in frequency shift as the mass of varnish added increased. In the case of the colophony-linseed oil varnish, this was better correlated than

the shellac-spirit varnish. This correlation may be because the colophony-linseed oil varnish permeates the wood to a deeper level, and thus alters the frequency to a greater extent than the shellac-spirit varnish. This is supported by the average frequency shift of the colophony-linseed oil varnish, which was $-17.6767\,\mathrm{Hz}\pm0.7004$, to the average frequency shift of the shellac-spirit varnish, which was $-5.0134\,\mathrm{Hz}\pm0.2467$.

A possible mechanism for this can be constructed as follows. The shellac-spirit varnish creates a thin, stiff film on top of the wood. This damps the plate to a greater extend than the colophony-linseed oil varnish, which is what the data shows. In fact, as more colophony-linseed oil varnish is added to the wood, the lower the attenuation rate. This means that more input energy is being outputted as sound energy. Fig. 6.1 (in Appendix) shows a graph of the frequency spectrum before and after the application of colophony-linseed oil varnish, and one can see that qualitatively, the average output in decibels actually increases as a result of being varnished.

In the case of the shellac-spirit varnish, the opposite is shown. As more shellac is deposited on the plate, the attenuation rate and damping coefficient both increase. This implies that less input energy is being transmitted as sound. Fig 6.2 (in Appendix) shows the exact opposite trend as Fig. 6.1; that is, the graph qualitatively shows that the average output in decibels decreases as a result of the application of shellac-spirit varnish.

The model given by the equation

$$\omega_2 = \omega_1\sqrt{\frac{d_1h_1}{d_2h_2}} \tag{10}$$

was shown to fit both the shellac-spirit and the colophony-rosin varnish. Both varnishes impart nearly opposite acoustic effects on the plates, yet this equation predicts both frequency shifts to a remarkable correlation ($R^2 = 0.9717$ and 0.9818). This lends significant support to proposing that this equation is a general formula for predicting frequency shifts, given the density of the plate and of the varnish, as well as a modal frequency.

where h_1 is the thickness of the plate before varnishing, h_2 is the thickness after varnishing, and m_w and m_v are the masses of the plate and varnish respectively. The intercepts for the plots obtained through this formula probably represent the approximate order of frequencies for which this equation is valid.

One interesting pattern is that as the varnish gets qualitatively stiffer, the plot for equation (6) drifts further away from a $y = x$ fit. this may be due to the stiffer varnish layer acting as a separate joined plate, resulting in a coupled plate system. Further theoretical work is required to examine this hyopthesis. By this idea, the plot for the colophony-linseed oil varnish remains closest to the $y = x$ fit since the varnish literally soaks deep into the wood, and in principle becomes part of the wood layer rather than making a separate layer.

Recall the model proposed by Farag and Pan (1998):

$$f_0 = \frac{1}{2\pi}([(\frac{m\pi}{a^2}) + (\frac{n\pi}{b^2})] \times \sqrt{\frac{D}{d_0h}}), \tag{11}$$

where m, n are wave numbers corresponding to 1/2 wavelengths (the mode driven in this experiment has $m, n = 2$), a, b are length and width, and D is the flexeural stiffness of the plate given by

$$D = \frac{Eh^3}{12(1-v^2)} \tag{12}$$

where E is the Young's modulus and v is Poisson's ratio of the plate. These are quantities easily measured by other experiments (Yoshihara and Tsunematsu, 2007).

Equation (6) can also be used to analitically study wave propagation in thin plates. These waves were originally studied by Horace Lamb, and are thus dubbed Lamb waves (Finch, 2005). They follow the set of differential equations:

$$\xi = \frac{\delta\varphi}{\delta x} - \frac{\delta\psi}{\delta z} \tag{13}$$

$$\zeta = \frac{\delta\varphi}{\delta z} + \frac{\delta\psi}{\delta x} \tag{14}$$

where the potentials φ and ψ obey wave equations $\ddot{\varphi} = c_l^2 \nabla^2 \varphi$ and $\ddot{\psi} = c_T^2 \nabla^2 \psi$ where c_l and c_T are the speeds of wave propagation in the length and thickness of the plate, respectively. Solutions of these differential equations are of the form

$$\frac{\tanh(\frac{h\sqrt{k^2 - \frac{4\pi^2 f_0^2}{c_l^2}}}{2})}{\tanh(\frac{h\sqrt{k^2 - \frac{4\pi^2 f_0^2}{c_T^2}}}{2})} = \frac{4k^2\sqrt{k^2 - \frac{4\pi^2 f_0^2}{c_l^2}}\sqrt{k^2 - \frac{4\pi^2 f_0^2}{c_T^2}}}{(2k^2 + \frac{4\pi^2 f_0^2}{c_T^2})^2}, \tag{15}$$

where k is the wave number. Using the proposed equation (6), the changes to the solutions of these equations as a result of varnishing the plate can be determined.

7 Conclusion

The frequency after the application of varnish on a rectangular plate of Engelmann Spruce was shown to follow the expression

$$f_2 = f_1\sqrt{\frac{d_1 h_1}{d_2 h_2}}, \tag{16}$$

where f_1 is the frequency of a mode before the application of varnish, d_2 is the plate density after varnish application and d_1 is the plate density before varnish application and h_2 and h_1 are the plate thicknesses before and after varnish application respectively.

These result have significance for the study of plate acoustics, as well as commercial value for companies such as musical instrument manufacturers.

8 Acknowledgments

Firstly, I would like to thank my mentor Professor Mark Van Raamsdonk for his excellent advice and guidance in pursuing this project. Professor Chris Waltham was a constant source of knowledge and expertise, and his help was invaluable in the completion of this paper.

I owe a debt of gratitude to David Webber of Webber Guitars, Inc. for sponsoring this project with the generous donation of high-quality Engelmann Spruce, and for allowing me to test and publish the results of his polyester guitar lacquer. I must also thank the talented Vincent Leung of the Center for Advanced Wood Processing for machining the wood. Lastly, but not least, I thank Dr. Irma Hoogendoorn for allowing me the use of the UBC Chemistry Laboratory's analytical balances, hot plates and fume hood.

9 References

Farag, N. H., and Pan, J. 1998. On the free and forced vibration of single and coupled rectangular plates. *Journal of the Acoustical Society of America.* **104**(1), 203-216.

Finch, R. D. 2005. *Introduction to Acoustics.* Upper Saddle River, New Jersey: Pearson-Prentice Hall.

Yoshihara, H., and Tsunematsu, S. 2007. Elastic properties of compressed spruce with respect to its cross section obtained under various compression ratios. Forest Products Journal. **57(4)**, 98-100.

Wolfram Alpha Computational Database. Retrieved from www.wolframalpha.com. Accessed March 2010.

10 Appendix

Error Propagation Formulae:

for $f = AB$ and $f = \frac{A}{B}$:

$$\delta f = \sqrt{(\frac{\delta A}{A})^2 + (\frac{\delta B}{B})^2} \tag{17}$$

Standard Error:

$$SE_x = \frac{\sqrt{\frac{1}{N}\sum(x_{bar} - x)^2}}{\sqrt{N}} \tag{18}$$

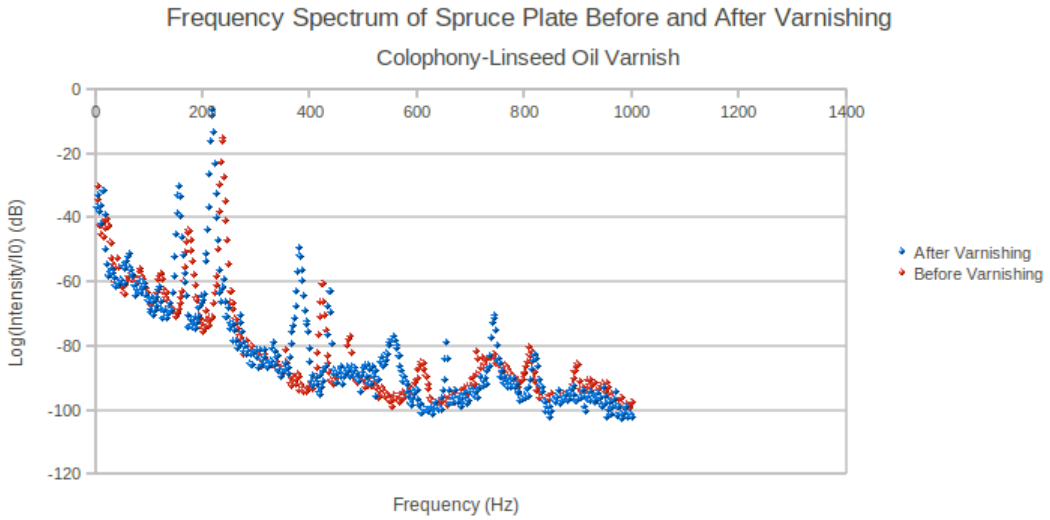

Figure 6.1: Average dB increases after varnishing.

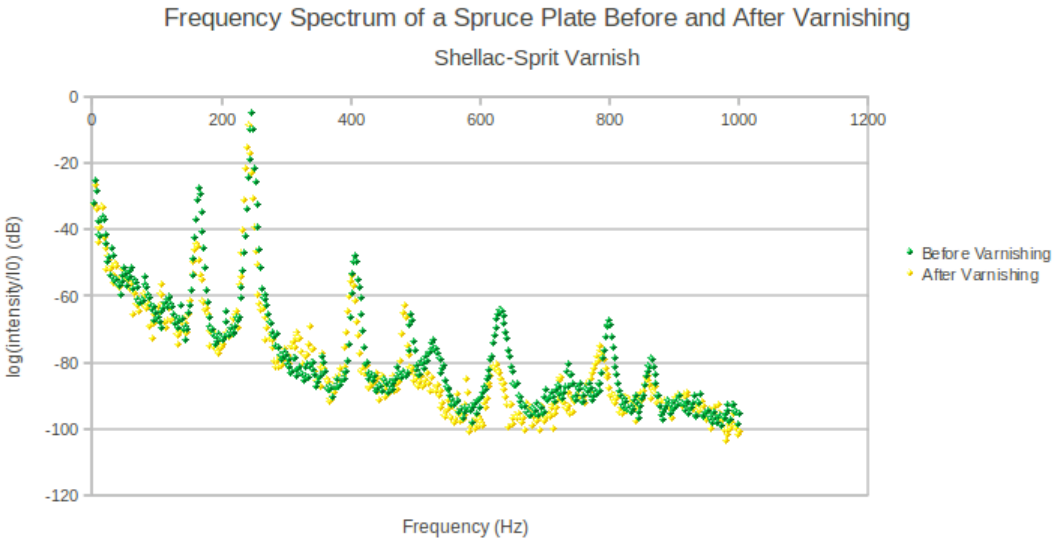

Figure 6.1: Average dB decreases after varnishing.